THE JOURNAL OF PHYSICAL CHEMISTRY B

ARTICLE

pubs.acs.org/JPCB

Raman Spectroscopic Signatures of Noncovalent Interactions Between Trimethylamine N-oxide (TMAO) and Water

Katherine L. Munroe,[†] David H. Magers,[*,‡] and Nathan I. Hammer[*,†]

[†]Department of Chemistry and Biochemistry, University of Mississippi, University, Mississippi 38677, United States

[‡]Chemistry and Biochemistry, Mississippi College, Clinton, Mississippi 39058, United States

Supporting Information

ABSTRACT: The effects of hydration on vibrational normal modes of trimethylamine N-oxide (TMAO) are investigated by Raman spectroscopy and electronic structure computations. Microsolvated networks of water are observed to induce either red or blue shifts in the normal modes of TMAO with increasing water concentration and to also exhibit distinct spectral signatures. By taking advantage of the selective and gradual nature of the water-induced shifts and using comparisons to theoretical predictions, the assignments of TMAO's normal modes are re-examined and the structure of the hydrogen-bonded network in the vicinity of TMAO is elucidated. Agreement between experiment and theory suggests that the oxygen atom in TMAO accepts on average at least three hydrogen bonds from neighboring water molecules and that water molecules are likely not directly interacting with TMAO's methyl groups.

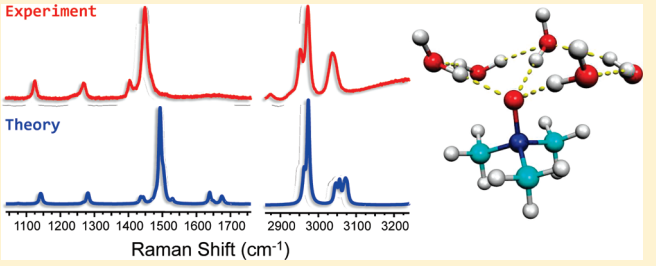

INTRODUCTION

Trimethylamine N-oxide (TMAO, shown in Figure 1) belongs to a small class of organic molecules called osmolytes, which have been studied extensively both theoretically and experimentally because they play important roles in biological functionality. TMAO promotes the folding of biopolymers, such as proteins and nucleic acids and also counteracts the denaturing effects of another osmolyte, urea, on the same biopolymers.[1,2] Even though TMAO demonstrates a substantial degree of hydrophobic character, it has been found to be highly soluble in water due to its high dipole moment. In fact, it has been suggested that osmolytes are effective because of their noncovalent interactions with solvated water molecules in biological media. In solution, hydrogen bonds between TMAO and water molecules are stronger than the hydrogen bonds present in pure water.[3,4]

Because of the importance of noncovalent interactions in biological media, such weak interactions have been the main focus in attempts to explain the molecular mechanism of the stabilizing effects of TMAO. However, to date the exact molecular mechanisms for the interactions between solvent, solute, and the protein have not been elucidated experimentally or theoretically due to the lack of a cohesive consensus.[2,5] This is in part due to the several complex reactions that are involved in the process of solvent, solute, and protein interactions.[6] Explanations for the molecular mechanism have been separated into two main types of hypotheses, termed "direct" and "indirect". These two terms are used loosely throughout the literature in either describing the mechanism or the interactions that are occurring. A direct mechanism or interaction is where the protein structure is changed (altered) by a direct interaction between the osmolyte and the protein (backbone) via electrostatic/van der Waals forces. An indirect mechanism is where the osmolyte interacts with water, altering the water structure, which then in turn changes the protein structure.[1,7] Since a change in the water structure by the osmolyte is a key component in the description of the indirect mechanism, the dipole moment of TMAO has also been an area of interest when looking at possible explanations of the molecular mechanism. This is because it is suggested that since TMAO has such a large dipole moment that it could alter the water structure.[8] However, there continues to be a significant disagreement in the literature over this issue.[9]

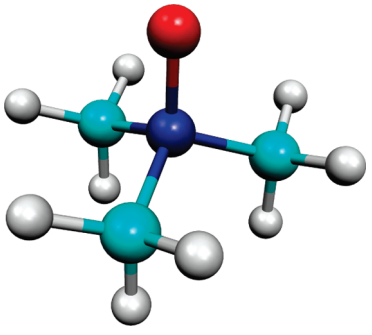

Figure 1. Molecular structure of trimethylamine N-oxide (TMAO).

Received: April 25, 2011
Published: May 20, 2011

dx.doi.org/10.1021/jp203840w | J. Phys. Chem. B 2011, 115, 7699–7707

Early spectroscopic studies involving TMAO concentrated on establishing its geometry and molecular properties. Properties of interest to these early researchers included TMAO's dipole moment, bond properties, force constants, and symmetry.[10−17] The dipole moment of TMAO has been studied extensively because of its magnitude being fairly large, indicating a semipolar bond.[10] Over the years TMAO's dipole moment has been measured and calculated by many different methods.[3,8,10,16,18−22] The N−O bond length is also of interest in characterizing the physical properties and behavior of TMAO.[3,14] Researchers are also interested in the physical properties of TMAO in the biological setting. Many spectroscopic studies, including infrared,[4,11,12,23−32] Raman,[5,14,15,33−35] NMR,[36,37] UV−vis absorption,[38] circular dichroism,[39−42] and gas electron diffraction[43] have been employed over the years to describe TMAO's molecular properties and help explain the effects of TMAO on hydrogen-bonded water networks and also biological environments in general.

Onori and Santucci have reported a number of vibrational spectroscopic studies[23,26−28,33] relating the effects of the mole fraction of TMAO to distortions in the hydrogen bond structure of water. In 2001 and 2002, they studied both the O−H stretching bands of water and the C−H stretching bands of TMAO using infrared spectroscopy.[23,27,28] Shifts in the C−H stretching bands could provide information on the self-aggregation of TMAO as a function of concentration. However, even though they observed a slight red shift (shift to lower energy) in the O−H stretching region of water, they did not see any effects on the C−H stretching bands of TMAO. The red shift in water's O−H stretches suggested the creation of stronger hydrogen bonds. In 2004, they studied effects of TMAO on water structure using near-infrared spectroscopy.[26] Sharp et al. also studied the effects of TMAO on water structure using infrared spectroscopy,[4] and in 2009 Panuszko et al. used isotopically labeled water (HDO) to study similar effects.[30] In the latter case, the authors showed that water interacting with TMAO formed stronger hydrogen bonds and exhibited a much more ordered hydrogen bonded network than pure water. Rezus and Bakker recently employed femtosecond mid-infrared pump−probe spectroscopy to study the effects of TMAO on the structural dynamics of neighboring water molecules.[24,25] By studying HDO, they observed a decrease in the vibrational relaxation rate of the OD vibration when the TMAO concentration was increased. They also observed an increase in the reorientation rate of water because of added defects in the extended hydrogen bonded network.

Even though there have been a number of vibrational spectroscopic studies involving TMAO and its stabilizing effects on proteins, there are few reports in the literature employing the use of Raman spectroscopy to study the noncovalent interactions between TMAO and water and water's effects on the solvated TMAO molecule. Raman spectroscopy offers complementary information to that obtained when using infrared-based methods. In many instances, Raman spectroscopy also offers opportunities to investigate the subtle effects of weak noncovalent interactions.[44,45] Early Raman studies of TMAO reported spectra in various solvents.[5,14,34,35] In 1937, Edsall reported the Raman spectra of the TMAO·HCl complex in aqueous HCl solution.[34] Goubeau and Fromme later measured the Raman spectra of anhydrous TMAO in methanol solutions and assigned modes based on comparisons with similar molecules.[35] In 1966, Kuroda and Kimura measured the Raman spectra of TMAO·$2H_2O$ in aqueous solutions.[14] Even though they measured the Raman spectrum of the dihydrate, they are the first to report a polarized Raman spectrum of TMAO. Polarized Raman spectra are valuable in assigning symmetries of normal modes. Raman-scattered light polarized perpendicularly to the incident laser polarization is less intense compared with the scattered light polarized parallel to the incident laser polarization for modes belonging to the totally symmetric irreducible representation, a_1. These authors also calculated the normal vibrations of TMAO using normal coordinate treatment. Using these calculations and the polarized Raman lines, they assigned symmetries to the observed frequencies and corrected assignments made earlier by Giguere and Chin,[11] who had employed infrared spectroscopy to study TMAO. Choplin and Kauffman later reported the Raman spectrum of solid TMAO in 1970 and also assigned normal modes.[15] These later assignments agreed with the conclusions made by Kuroda and Kimura.[14]

In 2006, Onori and Santucci employed Raman spectroscopy in an attempt to explain the hydrophobic effects of TMAO as a function of concentration.[33] This is the first and only report where noncovalent interactions between TMAO and water have been studied using Raman spectroscopy. Their goal was to explain the molecular mechanism of protein stabilization by TMAO in water and its ability to counteract urea. They studied the Raman spectra of water in the O−H stretching region as well as the C−H stretching band of TMAO in the 2900−3100 cm^{-1} region. These two regions were selected because the authors had previously studied the perturbation on the water structure using infrared[23,27,28] and near-infrared[26] spectroscopies. As in the case of the earlier infrared studies, the authors noticed only a slight red shift in the O−H stretching region and did not see any effects on the C−H stretching bands of TMAO.

Along with the many experimental investigations, a number of ab initio[3,8,21,30,43,46] and simulation (including molecular dynamics[6,7,9,22,29,30,37,46−60] and Monte Carlo[4,8]) studies have also been performed. In the 1990s, Haaland et al.,[43] Noto et al.,[46] and Kast et al.[21] first studied interactions between TMAO and water using ab initio methods. Haaland et al.[43] compared the earlier experimental Raman results by Choplin et al.[15] when developing their force field and scale factors. In 2004, Maclagan et. al employed many different computational methods to look at the interaction of water with TMAO.[8] Specifically, the authors were interested in the effects of TMAO (a compensatory solute) on the surrounding water structure and comparing that to the effects of noncompensatory solutes such as urea. However, based on the solute/water interaction energies, they saw no clear differences in the effects on the surrounding water structure between the compensatory solutes and the noncompensatory solutes.[8] More recently, in 2010 Wei et al. performed molecular dynamics simulations on TMAO-water clusters and reported that TMAO strengthens the hydrogen bonds between water molecules, significantly slows the orientational relaxation of water, and makes the hydrogen bond network more icelike.[7] The authors asserted that the methyl groups on TMAO are responsible for these effects. In fact, most of the recent theoretical studies have come to the conclusion that TMAO strengthens the hydrogen bonds of the surrounding water molecules. However, Kuffel and Zielkiewicz assert that this strengthening effect is very small.[9]

Most, if not all, of the previous experimental and theoretical studies involving TMAO's interactions with water have concentrated on perturbations in water's hydrogen bonded network. In

general, spectroscopic studies to elucidate water's structure simultaneously interrogate all of the water molecules within the probe volume at once, rather than just the waters directly interacting with TMAO.[61] In contrast, spectroscopically probing the properties of TMAO in the presence of water can reveal the structure of the local water network directly hydrogen bonded to TMAO. Also, for a complete understanding of the subtle interactions between TMAO and water, as well as TMAO's ability to stabilize proteins and counteract urea, an analysis of the effects on TMAO's properties when hydrated is also important in understanding these complex systems.[2] Here, we address these questions by reporting detailed Raman spectra of TMAO as it is solvated by water molecules starting with solid TMAO in an inert atmosphere to a final dilution of $\chi_2 = 0.000625$ in water, where χ_2 indicates the mole fraction of TMAO in aqueous solutions. We compare the experimental spectra to the results of electronic structure calculations performed on molecular clusters consisting of one TMAO molecule surrounded by up to eight water molecules.

EXPERIMENTAL AND THEORETICAL METHODS

Spectroscopic Methods. Commercial grade anhydrous trimethylamine N-oxide (Sigma-Aldrich) was used without further purification. The excitation sources employed for Raman spectroscopy were the 514.5 nm line from either a Coherent Innova 200 Ar ion laser or Spectra Physics 2018-RM Kr/Ar ion laser. The spectra were collected using a Jobin-Yvon Ramanor HG2-S Raman spectrometer with two 2000 grooves/mm gratings and a thermoelectrically cooled (−30 °C) photomultiplier tube detector. Scan speeds of 1 or 2 cm^{-1}/s were typically employed for spectra shown here. Spectra were obtained for the solid state of TMAO in a nitrogen environment. Time-resolved spectra of solid TMAO in a humid atmosphere (50% relative humidity) were obtained to qualitatively show the initial effects of microhydration of neat TMAO. Raman spectra of solutions of TMAO in water ($\chi_2 = 0.08 - 0.000625$) were obtained to monitor the further effects of increased dilution.

Theoretical Methods. Optimum equilibrium geometries and corresponding electronic energies of TMAO and TMAO with up to eight water molecules were determined using density functional theory.[62,63] The functional employed is the B3LYP hybrid functional comprising Becke's three parameter functional[64] using the LYP correlation functional of Lee, Yang, and Parr.[65] The basis set used is the augmented correlation consistent basis set aug-cc-pVTZ created by Dunning and co-workers.[66,67] Before it is augmented, this basis set uses a triple-ζ description for valence electrons and a single-ζ description for core electrons. Its polarization functions consist of two d and one f function for each carbon, nitrogen, and oxygen, and two p and one d function for each hydrogen. When augmented, diffuse s, p, d, and f functions are added to every non-hydrogen atom, and diffuse s, p, and d functions are added to each hydrogen atom. For calculations on TMAO surrounded by eight waters, this basis set results in 1,173 basis functions. On each optimized structure, vibrational frequencies and the corresponding Raman intensities were computed within the double harmonic approximation that treats molecules as multidimensional harmonic oscillators with linear electronic dipole moment functions. All of the electronic structure calculations were performed on a 16-core QuantumCube from Parallel Quantum Solutions using the PQS Ab Initio Program Package Version 3.3.[68] Simulated spectra were created by combining Lorentzians for each normal mode using a custom program developed with National Instruments LabView. The structures were chosen by considering numerous starting geometries, many of which converged to the same final structure. Because of the possible importance of interactions between water and methyl groups, many of these initial geometries had water molecules near and interacting with the methyl groups. However, in most cases water molecules did not remain near the methyl groups during the optimization process.

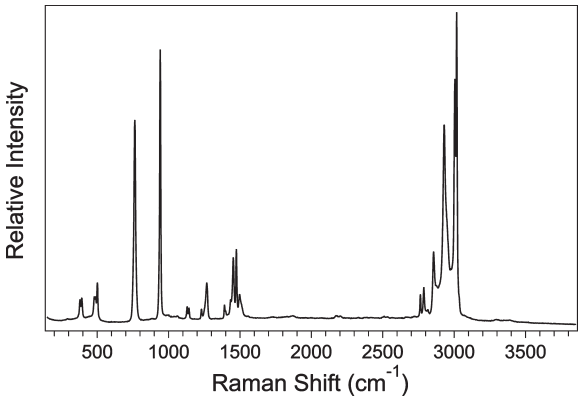

Figure 2. Raman spectrum of solid anhydrous TMAO under nitrogen.

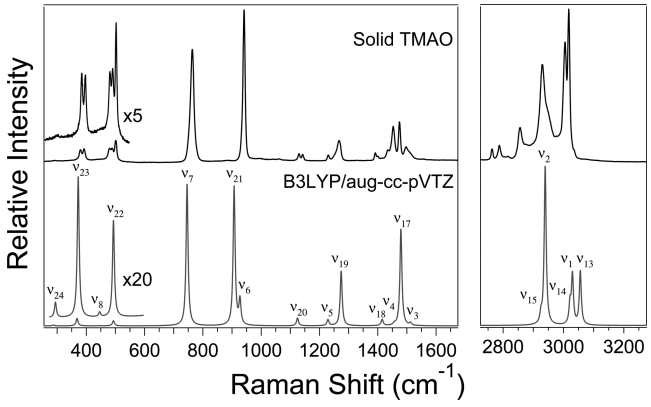

Figure 3. Raman spectrum of solid anhydrous TMAO compared to a simulated spectrum from B3LYP/aug-cc-pVTZ harmonic vibrational frequencies. Frequencies have been scaled by 0.964 in the C−H stretching region.

RESULTS

Spectroscopic Results. Figure 2 shows the Raman spectrum of solid anhydrous TMAO in a nitrogen environment. TMAO is very hygroscopic and readily forms a thin film of water within a few minutes in a humid atmosphere.[11] For this reason, care must be taken in obtaining the spectrum of anhydrous TMAO, and several previous authors have concentrated their efforts on the dihydrate species.[5,11,14,31,32] Here, we revisit the vibrational spectrum of anhydrous TMAO and examine how it is affected by the presence of water. Shown in Figure 3 is a comparison of the Raman spectrum of solid anhydrous TMAO compared to a simulated spectrum from B3LYP/aug-cc-pVTZ harmonic vibrational frequencies of an isolated TMAO monomer. Overall, there is very good agreement between the experimental solid phase

Table 1. Normal Modes of TMAO

			Giguere	Kida	Kuroda	Choplin	Haaland	current	current
mode	symm	motion	1961	1963	1966	1970	1991	Raman	B3LYP[a]
ν_1	a_1	C−H stretch			3038	3030	3030	3018	3030
ν_2	a_1	C−H stretch			2970	2948	2949	2952	2940
ν_3	a_1	CH_3 def			1482	1480	1479	1497	1512
ν_4	a_1	CH_3 def		1400	1398	1395	1390	1435	1455
ν_5	a_1	CH_3 rock		1245	1240	1255	1252	1231	1229
ν_6	a_1	N−O stretch	937	948	936	935	932	945	927
ν_7	a_1	C−N stretch	757	755	756	765	771	764	746
ν_8	a_1	skeletal def	490	464	469	466	460	448	441
ν_9	a_2	C−H stretch					2896		3049
ν_{10}	a_2	CH_3 def					1421		1455
ν_{11}	a_2	CH_3 def					1002		1059
ν_{12}	a_2	CH_3 Torsion					225		215
ν_{13}	e	C−H stretch			3038	3020	3021	3036	3055
ν_{14}	e	C−H stretch			3038	2900	2901	3006	3021
ν_{15}	e	C−H stretch			2970	2870	2866	2931	2926
ν_{16}	e	CH_3 def		1465	1472	1456	1459		1489
ν_{17}	e	CH_3 def			1457	1445	1450	1465	1479
ν_{18}	e	CH_3 def		1400	1398	1389	1389	1400	1414
ν_{19}	e	CH_3 rock		1245	1240	1241	1253	1268	1276
ν_{20}	e	CH_3 rock		1125	1124	1124	1121	1136	1123
ν_{21}	e	C−N stretch	945	941	946	945	941	945	905
ν_{22}	e	N−O rock	472	509	497	490	484	489	492
ν_{23}	e	CNC bend	378	383	380	364	378	386	367
ν_{24}	e	CH_3 Torsion					294	293	283

[a] C−H stretching frequencies have been scaled by 0.964 for comparison with experiments.

Raman spectrum and the simulated spectrum from the electronic structure calculations. TMAO has C_{3v} symmetry and possesses eight modes of a_1 symmetry, four modes of a_2 symmetry, and twelve modes of e symmetry. Modes of a_1 and e symmetry are Raman active, but modes of a_2 symmetry are not.

Peaks in the Raman spectrum of solvated and solid TMAO have previously been assigned[11,14,15,22,32] to normal modes and Table 1 summarizes these vibrational frequencies. Here, the comparison of the current higher resolution experimental spectra in an inert atmosphere (current Raman in Table 1) with theoretical results (current B3LYP) is used in confirming or updating these earlier assignments. Peaks in the calculated C−H stretching region have been scaled so that a meaningful comparison with experiment can be made. Four modes are expected to be present in the Raman spectrum below 600 cm^{-1}. Two of these modes (ν_8 and ν_{24}) are expected to be very weak but are evident in the experimental spectrum in Figure 3, very close to the expected energies. The other two modes (ν_{22} and ν_{23}) are of e symmetry and are observed to split into multiple peaks, which is common in crystalline solids. The mode ν_{24} at 293 cm^{-1} has previously not been observed experimentally, but was predicted by Haaland et al. in 1991.[43] Three peaks are expected between 600 and 1000 cm^{-1}, although two of these are expected to be very close in energy. In this range only two large peaks are in fact evident in the experimental spectrum.

Eight peaks should be present in the range 1000−1500 cm^{-1}. The agreement between experiment and theory in this region is again very good with ν_5, ν_{19}, and ν_{20} all appearing very close to the predicted energies. The observed spectral pattern exhibited by the remaining five modes appears very similar to that predicted by theory when splitting in the crystalline state is taken into account. This, however, contrasts earlier assignments found in Table 1. The most prominent peak in this region is expected to stem from the e mode ν_{17} and there is in fact a decent-sized doublet in the experimental spectrum near the expected location centered at 1465 cm^{-1}. Similarly, ν_{18}, another e symmetry mode, is also observed to split as well and is centered at 1400 cm^{-1}. Peaks are also observed at 1497 and 1435 cm^{-1} where the a_1 symmetry modes ν_3 and ν_4, respectively, are expected. Missing, however, is an assignment of ν_{16}, although this peak is expected to be very weak. Below, shifts induced by the presence of water help confirm these assignments.

Assignment of modes in TMAO's C−H stretching region is not straightforward as there are at least eleven peaks present in the solid phase experimental spectrum for just five Raman active fundamentals in this region. Splitting of modes and combination bands likely contribute to the complicated spectral features. Two of the five Raman active modes possess a_1 symmetry and three have e symmetry. In two cases, peaks of different symmetry are expected by theoretical predictions to be overlapped, making assignments even more complicated. The highest energy mode in this region is predicted to be ν_{13}, which has e symmetry. The next two modes are expected to lie close in energy and are ν_1 (a_1) and ν_{14} (e). The last two modes, ν_2 (a_1) and ν_{15} (e), are also expected to be very close in energy with ν_2 expected to have the highest intensity in the region. Soley on the basis of a comparison

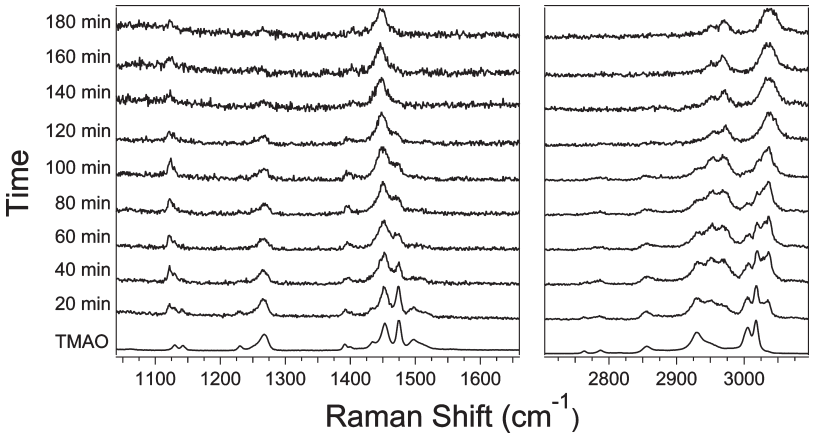

Figure 4. Raman spectra of solid anhydrous TMAO at various times after being exposed to an atmosphere of 50% relative humidity.

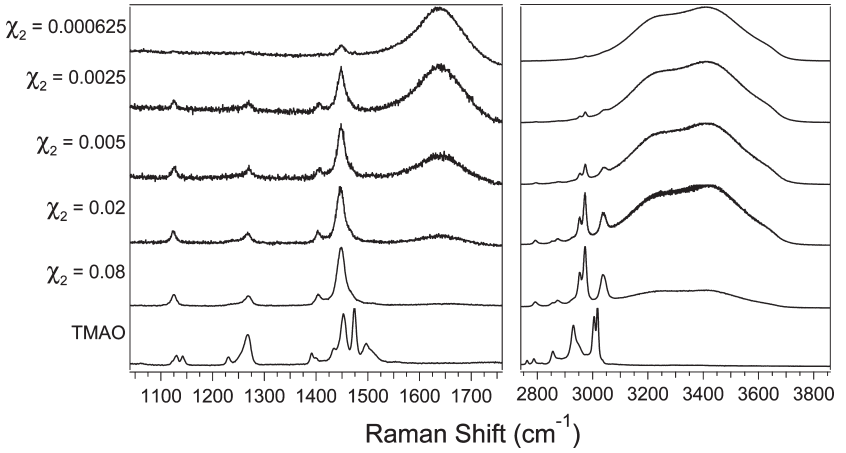

Figure 5. Raman spectra of aqueous TMAO solutions compared to that of solid anhydrous TMAO.

between experiment and theory, it is difficult to confirm previous assignments of modes without additional experimental information. Kuroda and Kimura[14] previously employed polarized Raman spectroscopy of the dihydrate in aqueous solution to aid in assigning these modes. As shall be shown below, however, the presence of water dramatically affects the normal modes of TMAO in this region. By taking advantage of this effect, assignment of C−H stretching fundamentals becomes possible.

Figure 4 shows Raman spectra of solid anhydrous TMAO at various times after being exposed to an atmosphere of 50% relative humidity. TMAO is very hygroscopic and readily forms a thin film of water within a few minutes in a humid atmosphere. In fact, after about two hours a few milligrams of TMAO becomes totally enveloped in a full drop of water that has deposited. Here, this effect is taken advantage of in order to monitor how the Raman spectrum of TMAO gradually evolves with hydration. The C−H stretching region is immediately affected by the presence of water with the highest energy peak at 3036 cm^{-1} becoming much more pronounced. Structure in the broad shoulder ranging from 2925−2975 cm^{-1} also emerges and by forty minutes exposure time two distinct peaks have emerged as dominant features in the spectrum. The overall effect is a blue shift in the experimental features in the region. In the CH_3 bending region of the spectrum (1350−1550 cm^{-1}), the opposite is true. Whereas there are multiple peaks in anhydrous TMAO, the addition of water reduces these features to one dominant peak centered at approximately 1450 cm^{-1}. The overall effect is a red shift of experimental features in this region. The significant exception, however, is that the peak assigned to ν_{18} at 1400 cm^{-1} does display a blue shift with time. These effects are studied further by acquiring the Raman spectra of aqueous TMAO solutions of known concentration, starting with a mole fraction of TMAO of approximately 0.08. Raman spectra of selected dilutions are presented in Figure 5 with additional spectra included in the Supporting Information. The mole fraction χ_2 = 0.08 represents a saturated solution of TMAO and is consistent with the solvated TMAO (top spectrum) in Figure 4. Further dilutions do not affect the Raman spectrum of TMAO except for new bands due to the Raman spectrum of liquid water. The water bend is evident at approximately 1650 cm^{-1} and the symmetric and asymmetric stretches appear at about 3200 and 3425 cm^{-1}, respectively. Onori and Santucci previously employed Raman spectroscopy with similar concentrations in an attempt to explain the hydrophobic effects of TMAO.[33] The authors noticed a slight red shift in the O−H stretching region of water with increasing TMAO concentration but did not see any effects on the C−H stretching bands of TMAO. This is consistent with the results presented here.

Theoretical Results. To aid in the analysis of the experimental observations, electronic structure computations were performed

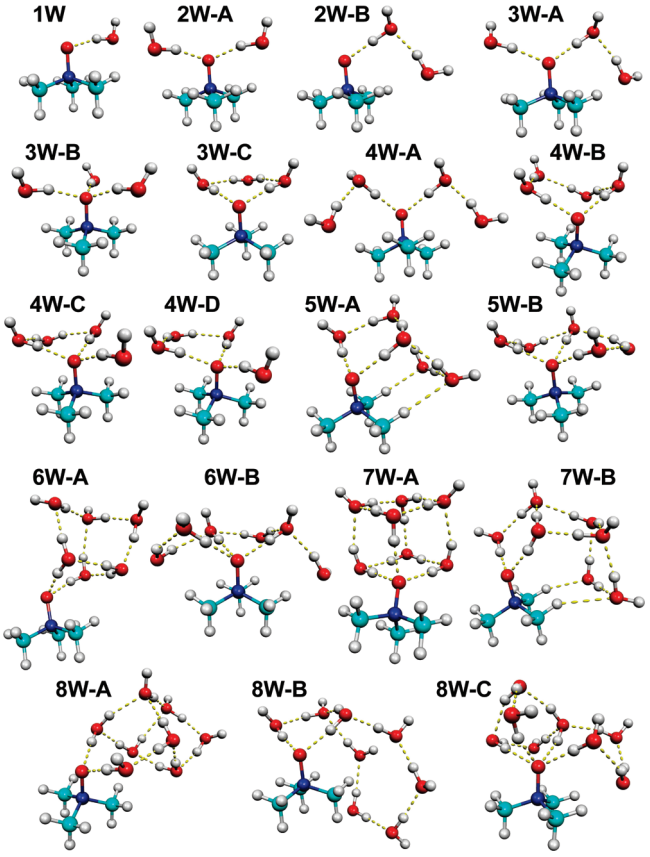

Figure 6. Optimized structures of TMAO with 1 to 8 water molecules.

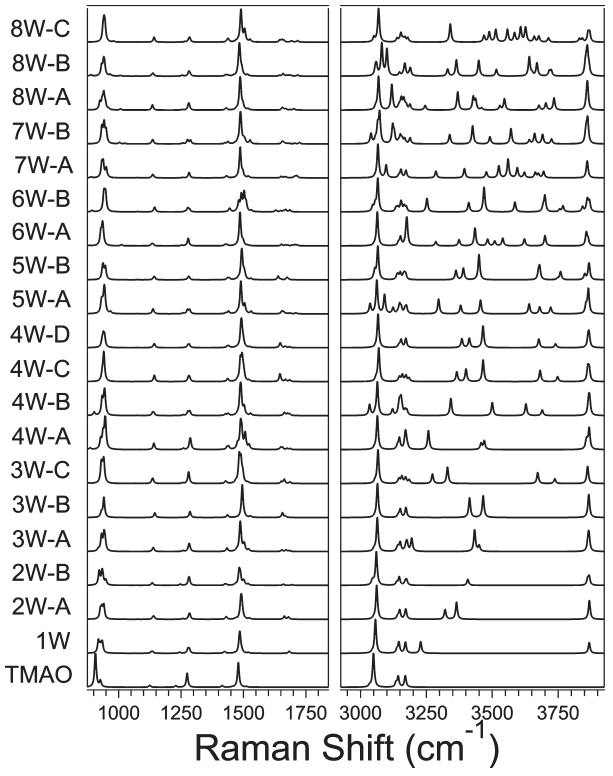

Figure 7. Simulated Raman spectra of TMAO/water solutions compared to that of an isolated TMAO molecule.

on a number of microhydrated clusters containing a TMAO monomer. Optimized equilibrium geometries of these clusters are shown in Figure 6, and simulated Raman spectra of these explicit structures are compared in Figure 7. Unsurprisingly, in all of the TMAO and water clusters, one or more water molecules form a hydrogen bond with the oxygen of the TMAO. Weak hydrogen bonding[69,70] between TMAO's hydrogen atoms and oxygen atoms on adjacent water molecules are also present in some of the larger clusters. These intermolecular interactions in turn affect the structure of TMAO. One result to note is the N−O bond distance. The B3LYP/aug-cc-pVTZ prediction of the N−O bond distance in TMAO is 136.5 pm. This distance is greater in each of the microhydrated clusters. In the structure with only one water (1W), it is 137.9 pm, and in structure 2W-B it is 138.0 pm; but in all of the other systems, the N−O bond distance is 138.5 pm or greater. This bond distance, however, does not continue to increase as more waters are added. In the structures we computed, this distance maximizes at 140.0 pm in structures 5W-B and 6W-B.

The computed energies, zero point energies, and relative energies for TMAO and all of the microhydrated clusters are presented in Table 2. These relative energies are used in Figure 6 in that the structures are ordered in increasing energy for a given number of water molecules. Note that structures with two hydrogen bonds to the oxygen of TMAO tend to be more stable than those with one or three. The exceptions to this trend are that 3W-B is more stable than 3W-C and 7W-A is more stable than 7W-B. In addition, only one stable structure was found with more than three hydrogen bonds to the central oxygen. This cluster is represented by 8W-C and has four hydrogen bonds to the oxygen of TMAO, but it is the relatively least stable system of any we found, lying 6.28 kcal/mol above the cluster represented by 8W-A.

It is also interesting to note the tilt of the water molecules around the central oxygen of TMAO in some of the smaller clusters. The optimized structure of TMAO has C_{3v} symmetry, yet when only one water is added, its tilt destroys all symmetry. The same is true for structure 2W-A. In fact, when these systems are forced to have C_s symmetry, the optimized structures each have an imaginary frequency. However, when three waters are added around the central oxygen, the tilt of the waters is the same in each resulting in C_3 symmetry in structure 3W-B. Yet, when an additional water molecule is placed between two waters hydrogen bonded to the central oxygen, both hydrogen atoms of the latter lie in the N−O− −H−O plane resulting in restored planes of symmetry. Thus, both 3W-C and 4W-C have C_s symmetry.

The simulated Raman spectra, shown in Figure 7, are observed to evolve with an increasing number of water molecules. At the same time, however, similar spectral signatures are observed with regards to how the individual water molecules bind to the central TMAO molecule. A good example of such a structural motif is represented in 4W-B, 5W-A, and 7W-B. These structures include weak hydrogen bonding that manifests itself in red shifted C−H stretches evident in Figure 7.

DISCUSSION

The smooth progression of the peaks with increasing water concentration together with the good agreement with theoretical predictions allows for assignments to be confirmed both in the CH_3 bending and C−H stretching regions of TMAO and for the hydrogen bonded water network in the direct vicinity to be elucidated. For example, Figure 8 shows a comparison of the

Raman spectrum from the $\chi_2 = 0.08$ solution with the simulated Raman spectrum of the 5W-B cluster. Agreement in both regions is very good, suggesting that the average interactions present in TMAO/water solutions adopt the hydrogen-bonded network present in this type of cluster. In this structural motif, three hydrogen bonds are donated to the oxygen atom on TMAO. The clusters 6W-B and 8W-C (which even has four hydrogen bonds to TMAO's oxygen atom) also possess this same structural motif and exhibit similar vibrational features. In the CH_3 bending region, the pattern of peaks involving TMAO allows for assignments of all modes and by tracking the evolution with decreasing water content back to solid TMAO, the identities in the anhydrous solid are identified. These are summarized in Table 1. The a_1 modes ν_3 and ν_4 are easily assigned as is the e mode ν_{18}. This last mode, ν_{18}, was observed as a doublet in the solid state but is clearly assignable when clustered with water. The other two e modes, ν_{16} and ν_{17}, are predicted to be close in energy. ν_{16} is predicted by theory to be very weak, however, and inspection of the doublet centered at 1465 cm^{-1} with increasing water suggests that these two peaks are in fact the split ν_{17}. This is supported by the strong similarity of the experimental and theoretical spectra shown in Figure 8. It is likely, therefore, that previous assignments of ν_{16} are questionable.

Table 2. Computed Energies, Zero Point Energies, and Relative Energies for TMAO and Microhydrated Clusters

structure	energy (au)	zero point energy (au)	ZPE corrected (au)	relative energy (kcal/mol)
TMAO	−249.72499	0.125	−249.60021	
1W	−326.20894	0.149	−326.05945	
2W-A	−402.69023	0.174	−402.51622	0.00
2W-B	−402.69019	0.174	−402.51574	0.30
3W-A	−479.16969	0.199	−478.97073	0.00
3W-B	−479.16938	0.199	−478.97067	0.04
3W-C	−479.16923	0.199	−478.97052	0.13
4W-A	−555.65116	0.224	−555.42721	0.00
4W-B	−555.65027	0.225	−555.42563	0.99
4W-C	−555.64780	0.224	−555.42363	2.25
4W-D	−555.64778	0.224	−555.42352	2.32
5W-A	−632.13391	0.251	−631.88279	0.00
5W-B	−632.12550	0.250	−631.87572	4.44
6W-A	−708.61300	0.277	−708.33582	0.00
6W-B	−708.60298	0.274	−708.32876	4.43
7W-A	−785.10063	0.304	−784.79675	0.00
7W-B	−785.09327	0.301	−784.79203	2.97
8W-A	−861.57699	0.328	−861.24935	0.00
8W-B	−861.57020	0.326	−861.24465	2.95
8W-C	−861.56564	0.326	−861.23934	6.28

Kuroda and Kimura[14] previously reported polarized Raman spectra of the dihydrate and noted that the peak at 2970 cm^{-1} was polarized and possessed a character, whereas the peak at 3038 cm^{-1} was depolarized. Here, at higher concentrations of water, the peak at 2970 cm^{-1} is observed as a doublet. Agreement between experiment and theory is again very good with the lower energy peak in the doublet corresponding to an asymmetric C−H stretch and the higher energy a symmetric C−H stretch involving all of the hydrogen atoms on all three CH_3 groups in TMAO. Although the relative intensitites of these two peaks change with additional water molecules, the motions remain the same with the lower energy being ν_{15} with e symmetry and the higher energy and more intense being ν_2 with a_1 symmetry. The increase in intensity of ν_2 upon microhydration suggests that this mode can exhibit a larger change in polarizability in the presence of water than in the solid state. The broad peak at 3040 cm^{-1} in Figure 8 turns out to be multiple (six in the case of structure 5W-B) overlapped CH_3 stretching modes in the theoretical spectrum. This broadening is made possible because interactions with water molecules increase the number of normal modes present in the newly formed molecular cluster.

In general, spectroscopic studies to elucidate water's structure in the vicinity of TMAO (or other osmolytes) simultaneously have interrogated all of the water molecules within the probe volume at once, rather than just the waters directly interacting with TMAO.[61] Here, in contrast the properties of TMAO in the presence of water are spectroscopically probed and as a result, the

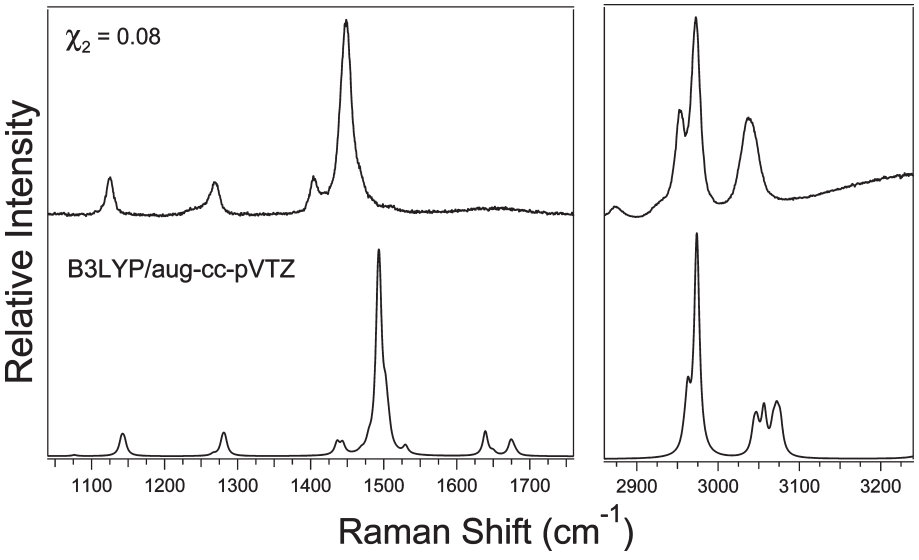

Figure 8. Simulated Raman spectrum of TMAO with five water molecules (5W-B) compared to that of a TMAO/water solution with molecule fraction $\chi_2 = 0.08$. The simulated C−H stretching peaks have been scaled by 0.97.

structure of the local water network directly interacting with TMAO is revealed. The result that TMAO likely hydrogen bonds on average to at least three water molecules is consistent with earlier theoretical predictions made by Athawale et al.[47] using molecular dynamics simulations. It is also consistent with conclusions made by a number of recent joint experimental/theoretical studies.[30,55,71] Panuszko et al. in a joint spectroscopic/theoretical study suggested that three water molecules are directly coordinated to the TMAO molecule and that additional water molecules hydrogen bond to these first three or surround the hydrophobic part of the molecule.[30] Meersman et al., who studied TMAO solutions using neutron scattering and theoretical methods, argued that the oxygen atom is strongly hydrogen bonded on average to two or three water molecules.[55] Also, they suggested that the hydrogen bonded water network is tighter than in pure water. Anand et al. studied TMAO's effects using self-assembled monolayers (SAMs) and molecular dynamics simulations and also argued that TMAO makes on average three hydrogen bonds with water.[71]

The results presented here also agree with recent observations made by Rezus and Bakker[24,25] that it is the hydrogen bonding by water with the terminal oxygen atom in TMAO that is key to its ordering of the extended hydrogen-bonded water network. As Zou et al.[60] pointed out, TMAO exhibits symmetry that is semispherical in nature and therefore creates different water structures at either end. At the hydrophilic end of the molecule, water molecules donate multiple hydrogen bonds to TMAO. However, these authors also reported a structured void near the methyl groups of TMAO suggesting that as shown in the current study that water preferentially bonds just to the oxygen in TMAO and that there are few interactions with the methyl groups. This structuring is likely the origin of the spectral shifts observed in TMAO. The blue shift observed here in the experimental C−H stretching region upon initial hydration is also observed in the theoretical spectra. Since very few molecular clusters involving weak C−H···O interactions were found as minimum energy structures, this result suggests that hydrogen bonding by water to the terminal oxygen atom has an important effect on TMAO's methyl groups and that a blue shift occurs even without direct interactions between TMAO's methyl groups and water. In contrast to the C−H stretching region, the CH_3 bending region of the spectrum (1350−1550 cm^{-1}) exhibited overall experimental red shifts in most modes. The various molecular clusters exhibited a wide range of shifts within these modes, depending upon the structural motifs present in the clusters. Interestingly, clusters that exhibit weak C−H···O interactions such as 5W-A and 7W-B exhibit the most blue-shifted C−H bends of all the clusters examined. On the other hand, 8W-B contains a very organized hydrogen-bonded network that protrudes into the vicinity of one of TMAO's methyl groups but does not directly interact through weak hydrogen bonds. This cluster exhibits among the lowest energy C−H bending modes of all the structures considered. The blue shift in ν_{18} in this region is also recovered in the theoretical calculations. These intriguing results suggest the notion of a void space around the methyl groups without direct interactions, as well as the formation of "iceberg water" in the surrounding solution.[24,72,73]

A number of authors have attempted to characterize this hydrophobic effect in water using a variety of different spectroscopic methods including neutron scattering,[55,74,75] NMR,[76,77] dielectric relaxation spectroscopy,[78,79] and the aforementioned infrared[4,23−28,30] and Raman spectroscopies.[33] Although earlier neutron diffraction studies were unable to show a difference between the structure of the water around hydrophobic groups of solutes and the bulk liquid, the NMR,[76,77] dielectric relaxation,[78,79] and certain vibrational spectroscopic studies[24,25,30] suggested solutions containing hydrophobic solutes, such as TMAO, exhibited a decrease in the average mobility of water molecules. In particular, Rezus and Bakker[24] suggested that iceberg water is not the ordered structure observed in ice, but rather that it resembles a disordered hydrogen bond network and that iceberg water is icelike from a dynamical perspective. The hydrophobic groups are surrounded by what are, in essence, immobilized waters. In TMAO, this effect originates from long-lived noncovalent interactions between TMAO's oxygen atom and water molecules. Good agreement between experiment and theory here suggests that at least three hydrogen bonds are directly involved in this indirect effect and that water molecules need not be interacting directly with TMAO's methyl groups to a substantial degree. TMAO's effectiveness as an osmolyte is likely a direct result of this restructuring of the water network in its immediate vicinity.

CONCLUSIONS

The effects of hydration on the normal modes of TMAO have been investigated using Raman spectroscopy and electronic structure computations. Whereas previous studies have concentrated their efforts on directly monitoring the properties of water in TMAO solutions, here, TMAO itself is interrogated. Raman spectra of 19 minimum energy structures composed of TMAO hydrogen bonded with 1−8 water molecules were computed and compared to the experimental results. By taking advantage of the selective and gradual nature of water-induced red and blue shifts and comparisons to the theoretical predictions, assignments of TMAO's normal modes were re-examined and important structural motifs were identified. Good agreement between experiment and theory also allows for the local hydrogen-bonded water network in the vicinity of TMAO to be elucidated. This agreement suggests that the oxygen atom in TMAO accepts on average at least three hydrogen bonds from neighboring water molecules and that water molecules are likely not interacting with TMAO's methyl groups to a substantial degree.

ASSOCIATED CONTENT

Supporting Information. Cartesian coordinates of the optimized TMAO/$(H_2O)_n$ clusters (n = 0−8) and additional Raman spectra of TMAO/water solutions. This material is available free of charge via the Internet at http://pubs.acs.org.

AUTHOR INFORMATION

Corresponding Author

*E-mail: (D.H.M.) magers@mc.edu; (N.I.H.) nhammer@olemiss.edu.

ACKNOWLEDGMENT

This work has been supported in part by the National Science Foundation (EPS-0903787 and CHE-0955550).

REFERENCES

(1) Bolen, D. W.; Rose, G. D. *Annu. Rev. Biochem.* **2008**, *77*, 339–362.
(2) Zhang, Y. J.; Cremer, P. S. *Annu. Rev. Phys. Chem.* **2010**, *61*, 63–83.

(3) Kocherbitov, V.; Veryazov, V.; Soderman, O. *J. Mol. Struct.* **2007**, *808*, 111–118.
(4) Sharp, K. A.; Madan, B.; Manas, E.; Vanderkooi, J. M. *J. Chem. Phys.* **2001**, *114*, 1791–1796.
(5) Kahovec, L. *Anz. Akad. Wiss. Wien* **1944**, *81*, 32–34.
(6) Yang, L.; Gao, Y. Q. *J. Am. Chem. Soc.* **2009**, *132*, 842–848.
(7) Wei, H.; Fan, Y.; Gao, Y. Q. *J. Phys. Chem. B* **2010**, *114*, 557–568.
(8) Maclagan, R.; Malardier-Jugroot, C.; Whitehead, M. A.; Lever, M. *J. Phys. Chem A* **2004**, *108*, 2514–2519.
(9) Kuffel, A.; Zielkiewicz, J. *J. Chem. Phys.* **2010**, *133*, 035102.
(10) Linton, E. P. *J. Am. Chem. Soc.* **1940**, *62*, 1945–1948.
(11) Giguere, P. A.; Chin, D. *Can. J. Chem.* **1961**, *39*, 1214–1220.
(12) Kida, S. *Bull. Chem. Soc. Jpn.* **1963**, *36*, 712–717.
(13) Caron, A.; Palenik, G. J.; Goldish, E.; Donohue, J. *Acta Crystallogr.* **1964**, *17*, 102–108.
(14) Kuroda, Y.; Kimura, M. *Spectrochim. Acta* **1966**, *22*, 47–56.
(15) Choplin, F.; Kaufmann, G. *Spectrochim. Acta, Part A* **1970**, *26*, 2113–2124.
(16) Armstrong, R. S.; Aroney, M. J.; Calderbank, K. E.; Pierens, R. K. *Aust. J. Chem.* **1977**, *30*, 1411–1415.
(17) Mak, T. C. W. *J. Mol. Struct.* **1988**, *178*, 169–175.
(18) Phillips, G. M.; Hunter, J. S.; Sutton, L. E. *J. Chem. Soc.* **1945**, 146–162.
(19) Tsygankova, N. G.; Bubel, O. N.; Grinshpan, D. D.; Kaputskii, F. N. *Vestsi Akad. Navuk BSSR, Ser. Khim. Navuk* **1988**, 35–37.
(20) Yakimanskii, A. V.; Bochek, A. M.; Zubkov, V. A.; Petropavlovskii, G. A. *Zh. Prikl. Khim. (Leningrad)* **1991**, *64*, 622–626.
(21) Kast, K. M.; Reiling, S.; Brickmann, J. *J. Mol. Struct.* **1998**, *453*, 169–180.
(22) Kast, K. M.; Brickmann, J.; Kast, S. M.; Berry, R. S. *J. Phys. Chem. A* **2003**, *107*, 5342–5351.
(23) Freda, M.; Onori, G.; Santucci, A. *J. Mol. Struct.* **2001**, *565*−*566*, 153–157.
(24) Rezus, Y. L. A.; Bakker, H. J. *Phys. Rev. Lett.* **2007**, *99*, 148301.
(25) Rezus, Y. L. A.; Bakker, H. J. *J. Phys. Chem. B* **2009**, *113*, 4038–4044.
(26) Di Michele, A.; Freda, M.; Onori, G.; Santucci, A. *J. Phys. Chem. A* **2004**, *108*, 6145–6150.
(27) Freda, M.; Onori, G.; Santucci, A. *J. Phys. Chem. B* **2001**, *105*, 12714–12718.
(28) Freda, M.; Onori, G.; Santucci, A. *Phys. Chem. Chem. Phys.* **2002**, *4*, 4979–4984.
(29) Stirnemann, G.; Hynes, J. T.; Laage, D. *J. Phys. Chem. B* **2010**, *114*, 3052–3059.
(30) Panuszko, A.; Bruzdziak, P.; Zielkiewicz, J.; Wyrzykowski, D.; Stangret, J. *J. Phys. Chem. B* **2009**, *113*, 14797–14809.
(31) Harmon, K. M.; Harmon, J. *J. Mol. Struct.* **1982**, *78*, 43–52.
(32) Mathis, R.; Wolf, R.; Gallais, F. *Compt. Rend.* **1956**, *242*, 1873–1876.
(33) Di Michele, A.; Freda, M.; Onori, G.; Paolantoni, M.; Santucci, A.; Sassi, P. *J. Phys. Chem. B* **2006**, *110*, 21077–21085.
(34) Edsall, J. T. *J. Chem. Phys.* **1937**, *5*, 225–237.
(35) Goubeau, J.; Fromme, I. *Z. Anorg. Chem.* **1949**, *258*, 18–26.
(36) Qvist, J.; Halle, B. *J. Am. Chem. Soc.* **2008**, *130*, 10345–10353.
(37) Sinibaldi, R.; Casieri, C.; Melchionna, S.; Onori, G.; Segre, A. L.; Viel, S.; Mannina, L.; De, L. F. *J. Phys. Chem. B* **2006**, *110*, 8885–8892.
(38) Kubota, T.; Yamakawa, M.; Tanaka, I. *J. Mol. Spectrosc.* **1966**, *20*, 226–232.
(39) Attri, P.; Venkatesu, P.; Lee, M.-J. *J. Phys. Chem. B* **2010**, *114*, 1471–1478.
(40) Baskakov, I. V.; Kumar, R.; Srinivasan, G.; Ji, Y. S.; Bolen, D. W.; Thompson, E. B. *J. Biol. Chem.* **1999**, *274*, 10693–10696.
(41) Vicky, D.-N.; Loria, J. P. *Protein Sci.* **2007**, *16*, 20–29.
(42) Atsushi, M.; Yuichi, K.; Kazufumi, T.; Shigenori, K. *Proteins: Struct., Funct., Bioinf.* **2008**, *71*, 110–118.
(43) Haaland, A.; Thomassen, H.; Stenstrm, Y. *J. Mol. Struct.* **1991**, *263*, 299–310.
(44) Howard, A. A.; Tschumper, G. S.; Hammer, N. I. *J. Phys. Chem. A* **2010**, *114*, 6803–6810.
(45) Wright, A. M.; Joe, L. V.; Howard, A. A.; Tschumper, G. S.; Hammer, N. I. *Chem. Phys. Lett.* **2011**, *501*, 319–323.
(46) Noto, R.; Martorana, V.; Emanuele, A.; Fornili, S. L. *J. Chem. Soc., Faraday Trans.* **1995**, *91*, 3803–3808.
(47) Athawale, M. V.; Dordick, J. S.; Garde, S. *Biophys. J.* **2005**, *89*, 858–866.
(48) Athawale, M. V.; Sarupria, S.; Garde, S. *J. Phys. Chem. B* **2008**, *112*, 5661–5670.
(49) Beck, D. A. C.; Bennion, B. J.; Alonso, D. O. V.; Daggett, V. *Methods Enzymol.* **2007**, *428*, 373–396.
(50) Bennion, B. J.; DeMarco, M. L.; Daggett, V. *Biochemistry* **2004**, *43*, 12955–12963.
(51) Biyani, N.; Paul, S. *J. Phys. Chem. B* **2009**, *113*, 9644–9645.
(52) Fornili, A.; Civera, M.; Sironi, M.; Fornili, S. L. *Phys. Chem. Chem. Phys.* **2003**, *5*, 4905–4910.
(53) Hu, C. Y.; Lynch, G. C.; Kokubo, H.; Pettitt, B. M. *Proteins: Struct,. Funct., Bioinf.* **2010**, *78*, 695–704.
(54) Laage, D.; Stirnemann, G.; Hynes, J. T. *J. Phys. Chem. B* **2009**, *113*, 2428–2435.
(55) Meersman, F.; Bowron, D.; Soper, A. K.; Koch, M. H. J. *Biophys. J.* **2009**, *97*, 2559–2566.
(56) Paul, S. *Chem. Phys.* **2010**, *368*, 7–13.
(57) Paul, S.; Patey, G. N. *J. Phys. Chem. B* **2006**, *110*, 10514–10518.
(58) Paul, S.; Patey, G. N. *J. Am. Chem. Soc.* **2007**, *129*, 4476–4482.
(59) Paul, S.; Patey, G. N. *J. Phys. Chem. B* **2008**, *112*, 11106–11111.
(60) Zou, Q.; Bennion, B. J.; Daggett, V.; Murphy, K. P. *J. Am. Chem. Soc.* **2002**, *124*, 1192–1202.
(61) Guo, F.; Friedman, J. M. *J. Phys. Chem. B* **2009**, *113*, 16632–16642.
(62) Hohenberg, P.; Kohn, W. *Phys. Rev. B* **1964**, 864–871.
(63) Kohn, W.; Sham, L. J. *Phys. Rev. A* **1965**, 1133–1138.
(64) Becke, A. *J. Chem. Phys.* **1993**, *98*, 5648–5652.
(65) Lee, C.; Yang, W.; Parr, R. *Phys. Rev. B* **1988**, *37*, 785–789.
(66) Dunning, J.; T., H. *J. Chem. Phys.* **1989**, 1007–1023.
(67) Kendall, R. A.; Dunning, T. H.; Harrison, R. J. *J. Chem. Phys.* **1992**, 6796–6806.
(68) *PQS Ab Initio Program Package*, Version 3.3; Parallel Quantum Solutions: Fayetteville, Arkansas, 2007.
(69) Jeffrey, G. A. *An Introduction to Hydrogen Bonding*; Oxford University Press: Oxford, England, 1997.
(70) Desiraju, G. R.; Steiner, T. *The Weak Hydrogen Bond in Structural Chemistry and Biology*; Oxford University Press: New York, 1999.
(71) Anand, G.; Jamadagni, S. N.; Garde, S.; Belfort, G. *Langmuir* **2010**, *26*, 9695–9702.
(72) Frank, H. S.; Evans, M. W. *J. Chem. Phys.* **1945**, *13*, 507–532.
(73) Tanford, C. *The Hydrophobic Effect*; Wiley: New York, 1980.
(74) Turner, J.; Soper, A. K. *J. Chem. Phys.* **1994**, *101*, 6116–6125.
(75) Buchanan, P.; Aldiwan, N.; Soper, A. K.; Creek, J. L.; Koh, C. A. *Chem. Phys. Lett.* **2005**, *415*, 89–93.
(76) Haselmeier, R.; Holz, M.; Marbach, W.; Weingaertner, H. *J. Phys. Chem.* **1995**, *99*, 2243–2246.
(77) Ishihara, Y.; Okouchi, S.; Uedaira, H. *J. Chem. Soc., Faraday Trans.* **1997**, *93*, 3337–3342.
(78) Kaatze, U.; Gerke, H.; Pottel, R. *J. Phys. Chem.* **1986**, *90*, 5464–5469.
(79) Wachter, W.; Buchner, R. *J. Phys. Chem. B* **2006**, *110*, 5147–5154.